ISSN:1687-1006

The Egyptian International Journal of Engineering Sciences and Technology

Vol. 33 (2021)17–27

https://eijest.journals.ekb.eg/

Numerical Study of Unstiffened Cold-Formed Steel Apex Moment Connection

Reda M. Ghamry [a*], Hassan M. Maaly[b], Ehab B. Matar [c],Ossama M. Elhossieny [d]

[a] *Assistant Lecturer at Structural Engineering Dept, Faculty of Engineering, Zagazig University, Zagazig, Egypt*
[b] *Associate Professor at Structural Engineering Dept, Faculty of Engineering, Zagazig University, Zagazig, Egypt*
[c] *Professor of Steel Structures , Faculty of Engineering, Zagazig University, Zagazig, Egypt*
[d] *Professor of Steel Structures , Faculty of Engineering, Zagazig University, Zagazig, Egypt*

ARTICLE INFO

Keywords:

1st Bolted Moment Connection
2nd Cold Formed Section
3rd Apex Connections

ABSTRACT

Cold-Formed Steel sections are commonly used in residential and commercial buildings as purlins, side girts, portal frames and moment resisting frames. The bolted moment connections can be used to connect the different structural components of these buildings together. These connections allowing the transfer of the internal forces of the structures such as axial forces, shear forces, bending moments and torsion. The main objective of this paper is to study numerically the behaviour of the apex bolted moment connection for cold formed sections. The deflection and the stress distribution at critical sections for unstiffened 2C (double back-to-back) CFS were investigated for two cases. Connecting single gusset plate was used in the first case, while two connecting double gusset plates in the second case. A finite element modelling was developed by using the ANSYS workbench to simulate the apex connection of cold-formed steel sections. The considered beams had span lengths of 4000 mm with nominal web depths of 150 mm and wall thickness 2.0 mm. A numerical model was developed and verified using the experimental results. The parametric study was carried out to investigate the effect of connecting gusset plate thickness, bolts patterns, and bolts pretension force on the resistance of the cold-formed steel sections. Based on this analysis the deflections, ultimate failure load, failure modes of specimens were studied and different failure modes, including local yielding in cold formed section, flexural-distortional buckling in the connecting gusset plate, and bearing failure near bolts are observed. Moreover, moment resistance ratio and rotations for this type of connection are deduced.

1. Introduction

Due to their light weight, durability and high structural performance cold-formed steel sections (C.F.S) were well suited for building construction. They are increasingly being used as beams and columns in low to medium rise building construction and medium span portal frames. The design guidance of cold-formed steel structures can be found in several codes of practice (AISI 2016 [1], AS/NZ 4600:1996 [2], BS5950-1998) [4]. Design recommendations on cold-formed steel section connections are mostly focused on the load carrying capacities of individual fasteners such as bolts, screws, rivets and spot welds. However, there is a shortage in a guidance on the structural performance

* Corresponding author. Tel.: +2-01119733008
E-mail address: drredagh@gmail.com

of the bolted moment connections for cold-formed steel sections .Lim & Nethercot -2003 [5], Dubina & Zaharia-1997 [6], Dubina -2008[7], Chung & Lau-1999 [12], Yu, Chung &Wong -2005 [10] , Chung, Yu & Wang -2005 [11] , Rinchen &Rasmussen-2019 [18] and El Aghoury ,et al-(2020) [19] reported experimental and analytical testing on bolted moment connections for cold-formed double channel sections.

In this paper, a numerical analysis is presented to study the behaviour and strength of bolted apex connections in cold –formed steel frames. Double unstiffened cold-formed channel beams are connected with two type of gusset plates using transfer web bolts. Several parameters are investigated. Moreover, different failure modes are discussed.

2. Verification by Finite Element Model

J.B.P. Lim and D.A. Nethercot [5] tested stiffened 2C-sections back to back with apex connection beam formed by using brackets bolted to the webs of the section to evaluate the deflection behavior of connection due to bending only. The results were continued until failure load and the mode of failure of each test was illustrated. The specimens were tested where their bracket dimensions are shown in Table (1). Fig. (1) shows the details of lateral restraint and load position, Fig. (2) shows gusset plate cross-section, Fig. (3) shows the dimensions of tested section and Fig. (4) shows dimensions of the connections A&D.

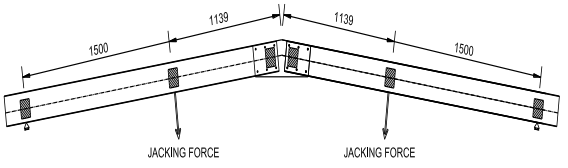

Fig. 1. Details of Lateral Restraint and Load Position

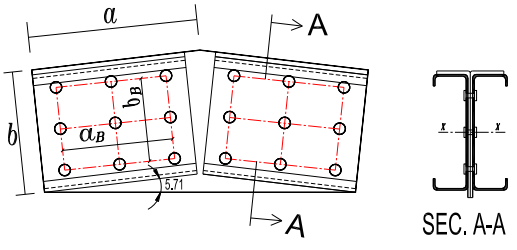

Fig. 2. Gusset Plate Elevation and Cross-Section

Table. 1. Dimensions of Connecting Gusset Plate

Test	Bracket a (mm)	b (mm)	t (mm)	Bolt –group a_B(mmm)	b_B(mm)
A	525	340	3.98	315	230
D	825	340	3.98	615	230

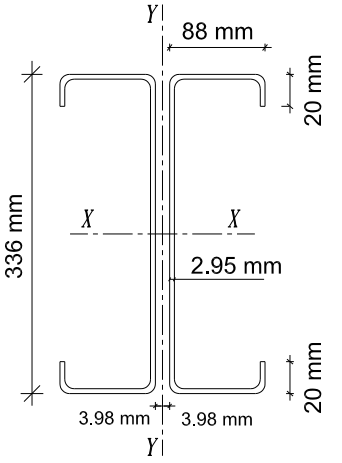

Fig. 3. Dimensions of Tested Channel-Sections

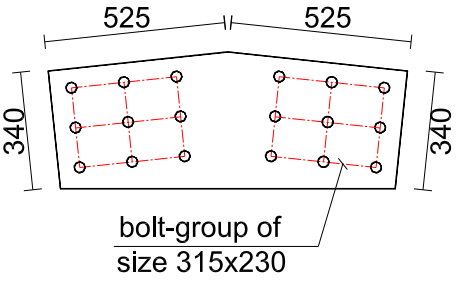

a) Joints (A)

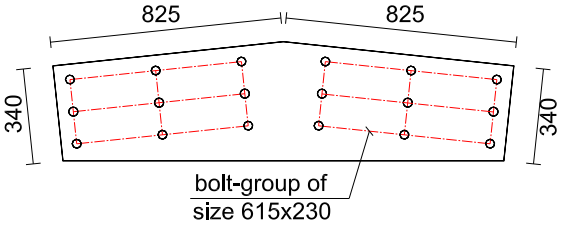

b) Joints (D)

Fig .4. Dimensions of Connecting Gusset Plates

2.1 Material properties

The properties of the tested beams and gusset plates were as the following:-

The average yield stress 358 N/mm^2 and the average ultimate stress 425 N/mm^2 for the channel section and, the average yield stress 341 N/mm^2 and the average ultimate stress 511 N/mm^2 for the gusset plates.

2.2 Validation of Numerical Model

The developed numerical model is to simulate the experimental specimens by using the finite element code ANSYS Workbench v19.2 [3] and predict the load- deflection curves and investigate the different failure modes. The following finite element were used to simulate the different structural elements,

1-SHELL181 elements were used for the 3D modeling of cold-formed steel channel.

2-SOLID186 elements were used for the simulation of the other connection parts i.e. (plates and bolts).

3-CONTA174 elements were used for 3D contact between different parts of connection.

Two specimens of section dimensions were modeled using F.E.M (ANSYS Workbench v19.2), the results are plotted together with the experimental data in Figures (5) and (6).Quarter model were used and symmetrical constraints were used to simulate a full model scale.

The graphs indicated that the F.E.M models agree with the experimental work for each specimen with acceptable accuracy. These figures show the relation between deflection and moment, where the deflection increases by increasing the load up to the failure. The failure load increase by increasing the gusset plate length as shown in joint D and the deflection decrease when the gusset plate increase also therefore, the failure load for joint A is less than joint D due to the decrease of gusset plate length. Fig. (5) shows the moment-deflection for joint A and Fig. (6) shows the moment-deflection for joint D. The deflection was measured at mid span of the beam.

Lim and Nethercot [5] noted that in their paper, the initial gradual increase in the gradient of the experimental moment–deflection curve of Connection (A) was reported to be attributable to imperfect alignment of the bolt holes and slack in the loading rods. Hence, this experimental curve was modified by first determining the connection stiffness at a bending moment of 40 kN. m, extending the curve down from this point to the horizontal axis with the same stiffness, and then shifting the curve to the origin.

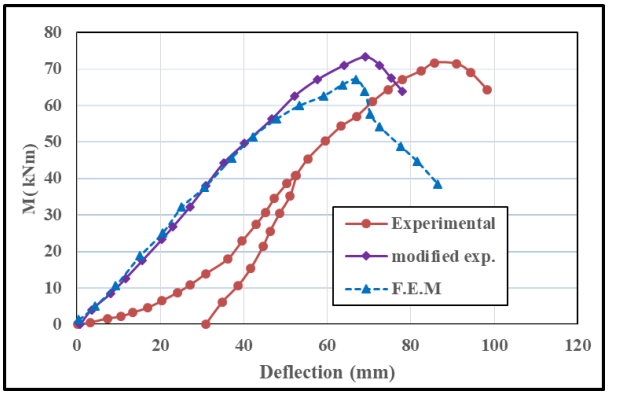

Fig. 5. Moment - Deflection Curve for Joint (A)

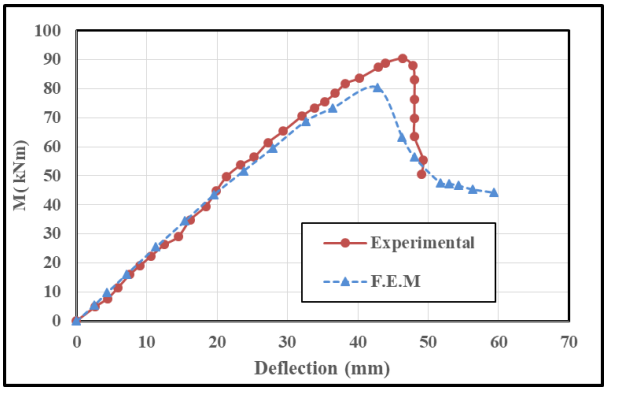

Fig. 6. Moment - Deflection Curve for Joint (D)

The experimental failure [5] occurred due to flexural buckling of the section as shown in Fig. (7) is similar to that occurred by the developed numerical model Fig. (8).

Fig.7. Experimental Channel Buckling Failure

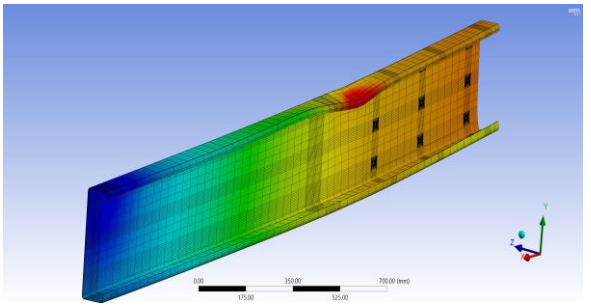

Fig. 8. Channel local Buckling Failure for F.E. Model

Table .2. Values of Maximum Deflection and Load VS. Test results.

Joint No	Exp. Def. (mm)	F.E.M Def.(mm)	Def. ratio	Exp. Moment (kN.m)	F.E.M Moment (kN.m)	Load ratio
A	91.02	83.27	0.915	71.46	65.6	0.918
D	46.3	42.70	0.922	90.4	80.45	0.89

A comparison between developed numerical model results and the experimental test results is listed in Table (2).An acceptable differences could be noticed. Generally, this acceptable difference in deflection could be testified as the experimental specimen is more flexible than the F.E.M due to the hole clearance between the bolt shaft with the plates and channel section.

3. Parametric Study

In this study two types of connections are considered, the first case is the single web gusset plate only, while the second case is doubled gusset plates with cutting compression flange. In all cases the variable thickness of gusset plate, different bolt group and variable tightened bolt forces were used to predict the effects of these parameters on the efficiency of the connection behavior. The load-deflection curves and the failure mode for each case were illustrated for the tested unstiffened 2C (double back-to-back) section.

3.1 Model Specifications.

The tested specimens consisted of two channels back to back with dimensions shown in Fig. (9). All models connection were connected together by non-pretension bolts, except three models were connected with pre-tensioned bolts (HSB) bolts with variable pretensioning force values 20%, 40% and 60% from the bolt pretension load. The young's modulus of the elasticity, E, and the yield stress F_y, of the steel material are considered as 210000 MPa and 360 MPa respectively. However, the yield stress, F_y, of the transfer bolts (M8) is considered as 640 MPa with a grade (8.8).The total length between the supports of the beams is 4000 mm with angle of inclination 6 degrees with horizontal. The right support was roller support and the left was hinged support. The steel used for beams and gusset plates is of yield stress 360 N/mm^2.

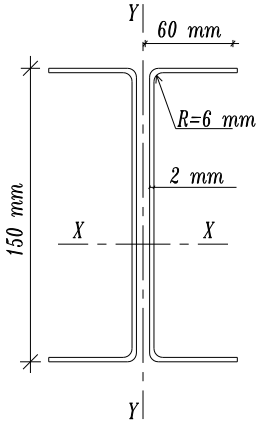

Fig. 9. Typical Dimensions of Modeled Section

Four 200*100 mm plates were added between the beam web (two at end supports and two at the quarter points of the beam span) and having the same thickness of the apex connection gusset plate. Lateral supports are used to prevent lateral torsional buckling of the beam each 100 cm as shown in Fig. (10).

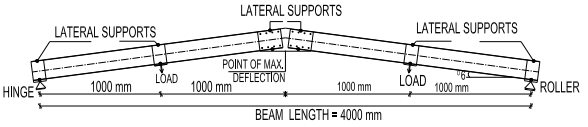

Fig. 10. Geometry of Modeled Beam and Load Position

The effective properties of the modeled single channel section in this study according to the AISC specification are as the followings:

I_x = 152.403 cm^4 , I_y = 11.794 cm^4

Area= 4.82 cm^2 ,

S_x (Elastic Section Modulus) = 18.42 cm^3

Z_x (Plastic Section Modulus) = 24.43 cm^3

The connecting gusset plate were modeled with bolt groups as shown in Fig.(11) with variable thickness 4, 5 and 6 mm for case of single plate and plate thicknesses 2 , 2.5 and 3 mm for case of double gusset plates.

The modeled beams properties are listed in Table (3) for the connection with single gusset plate and Table (4) for the connection with double gusset plates. The cross section geometry of the used gusset plates are illustrated in Figures (12.a &12.b).

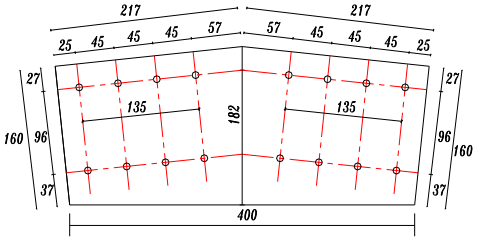

Bolt Group (4x2)

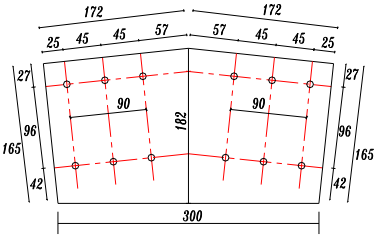

Bolt Group (3x2)

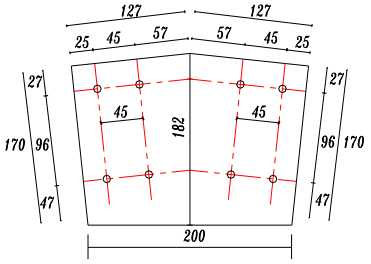

Bolt Group (2x2)

Fig. 11. Dimensions of Bolt Groups

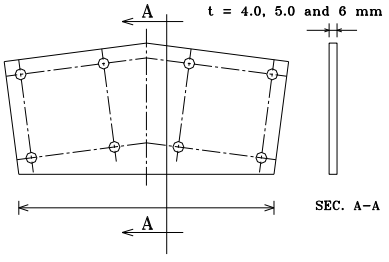

Fig. 12.a. Single Gusset Plate

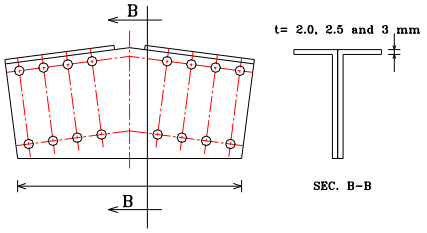

Fig. 12.b. Double Gusset Plates with Compression Flange

Table .3. Modeled Beams Properties for Single Gusset Plate

Model (NO)	Plate length (mm)	Plate Thickness (mm)	Bolt group	Pretension Force ratio
B1	400	6	4x2	-
B2	300	6	3x2	-
B3	200	6	2x2	-
B4	400	5	4x2	-
B5	400	4	4x2	-
B6	400	6	4x2	20%
B7	400	6	4x2	40%
B8	400	6	4x2	60%

Table .4. Modeled Beams Properties for Double Gusset Plates

Model (NO)	Plate length (mm)	Plate Thickness (mm)	Bolt group	Pretension Force ratio
B9	400	3	4x2	-
B10	300	3	3x2	-
B11	200	3	2x2	-
B12	400	2.5	4x2	-
B13	400	2	4x2	-
B14	400	3	4x2	20%
B15	400	3	4x2	40%
B16	400	3	4x2	60%

Figure (13) shows the 3-D model of the beam and Fig. (14) shows the refining of the finite element mesh around the bolt hole to improve the results of stress and deformation.

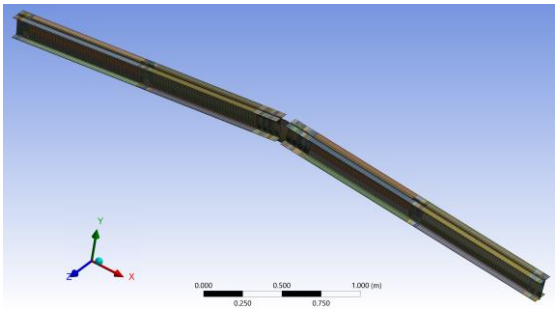

Fig. 13. 3-D View of Modeled Beam

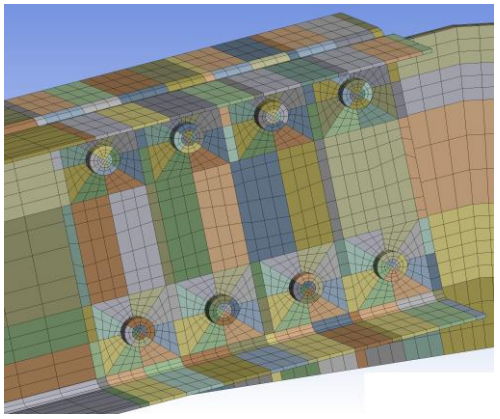

Fig. 14. Refining the Mesh around the Bolt Hole

3.2 Unstiffened Channel with Single Gusset Plate.

In this study using unstiffened channel section (beam) connected with single gusset plate was modeled to study the effect of bolt group geometry, plate thickness and bolts pretension force on the connection behavior. Table (5) shows the values of maximum deflection at max failure load and maximum failure load of modeled beams.

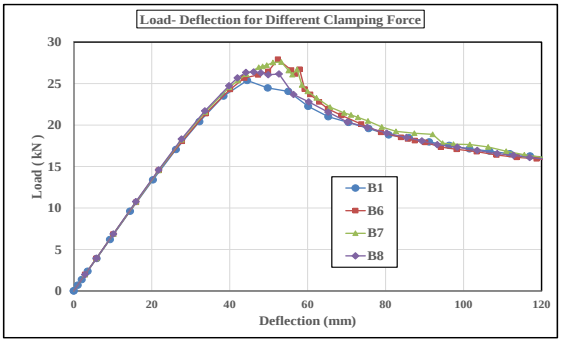

Fig.17. Load-Deflection for B1, B6, B7and B8

Figure (15) shows the load deflection relation at mid span with different thicknesses of gusset plate for B1, B4 and B5. The failure load are equals 25.4 kN, 24.1 kN and 23.5 kN and the deflection equals 44.5, 44.8 and 46.9 mm for plate thickness 6, 5 and 4 mm respectively. The difference in failure load and

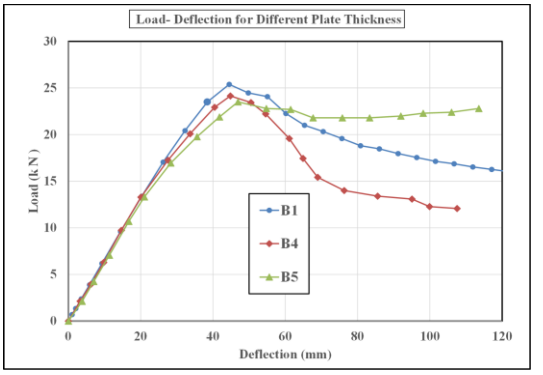

Fig.15. Load-Deflection for B1, B4 and B5

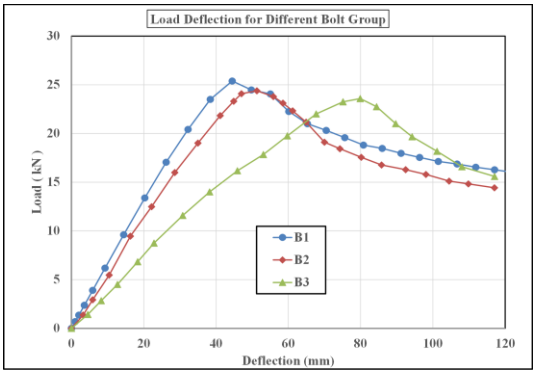

Fig.16. Load-Deflection for B1, B2 and B3

deflection between plate thicknesses for 5 and 6 mm is small because the failure occurs in the channel section as shown in Fig. (18), however the failure was in the connecting plate for thickness 4 mm as shown in Fig (19).

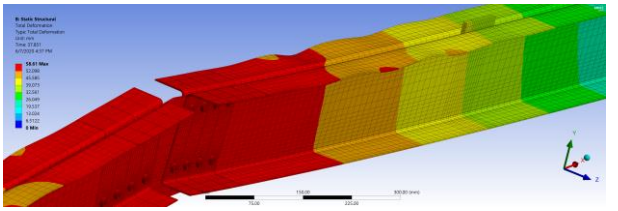

Fig.18. Buckling of Channel section for B1 and B4

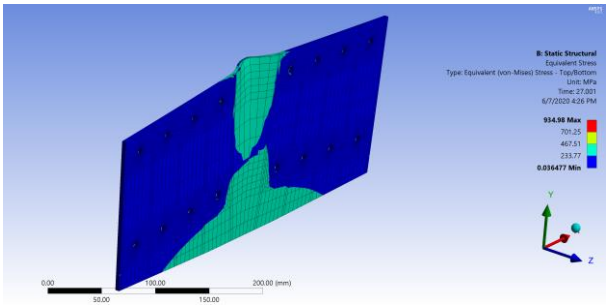

Fig.19. Buckling of Gusset Plate for B5

Figure (16) shows the load-deflection curve for different bolt group for B1, B2 and B3. The failure loads were equal to 25.4, 24.4 and 23.6 kN and the deflection values were equal to 44.5, 51.3 and 79.9 mm for bolt group 4x2, 3x2 and 2x2 respectively. The large plate length with the same pitch of bolt enhanced the beam deflection behavior however it has a small effect on the failure load due to bearing failure in the case of small bolt group such as 2x2.

Figure (17) shows the load-deflection curve for different beams for B1, B6, B7 and B8 for different pretension force. For the pretension loads of 20% and 40%, the failure loads were 9.8%, 8.6 % larger than non-pretension beam B1, respectively. The failure happened due to the buckling of gusset plate similar to B5 as shown in Fig. (19).The increasing of pretension force reduces the efficiency of the connection because of the initial imperfection that occurs in the thin plates. The failure was due to channel buckling as shown in Fig. (20).

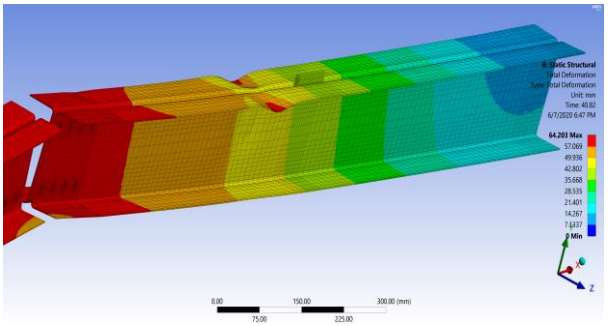

Fig.20. Buckling of Channel Section for B6, B7 and B8

Table .5. Values of Maximum Deflection and Maximum Load of Modeled Beams

Model (No)	maximum deflection at failure load (mm)	deflection ratio Bi/B1	maximum failure load (kN)	Load ratio Bi/B1
B1	44.5	1	25.4	1
B2	51.3	1.293	24.4	0.997
B3	79.9	1.67	23.6	0.834
B4	44.8	1.152	24.1	0.947
B5	46.9	1.268	23.5	0.865
B6	53.4	1.20	27.9	1.098
B7	53.3	1.19	27.6	1.086
B8	52.7	1.18	26.1	1.027

3.3 Unstiffened Channel with Double Gusset Plates having Compression Flange.

In this study unstiffened channel section with two gusset plates having compression flange is used to study bolt group geometry, plate thickness and pretension force on the connection behavior. Table (6) shows the values of maximum deflection at max. failure load and maximum failure load of modeled beams.

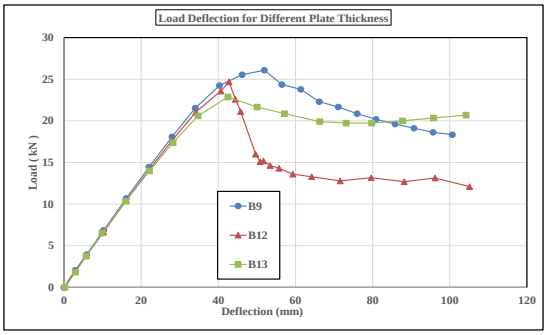

Fig.21. Load-Deflection for B9, B12 and B13

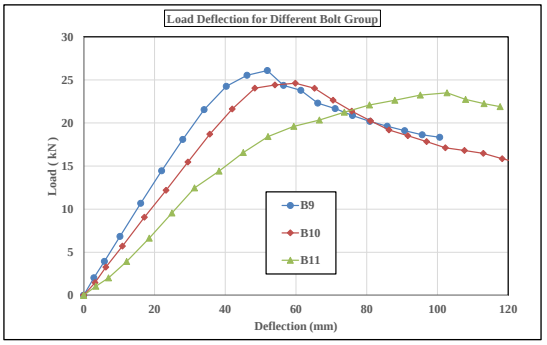

Fig.22. Load-Deflection for B9, B10 and B11

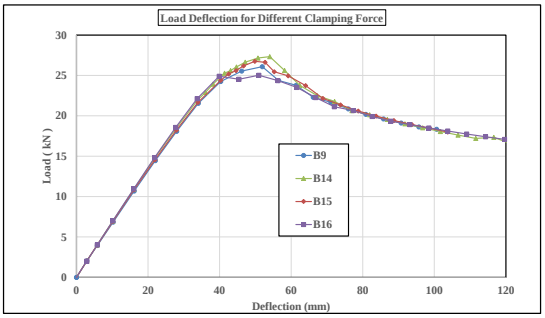

Fig.23. Load-Deflection for B9, B14, B15 and B16

Table .6. Values of Maximum Deflection and Maximum Load of Modeled Beams

Model (No)	maximum deflection at failure load (mm)	deflection ratio Bi/B9	maximum failure load (kN)	Load ratio Bi/B9
B9	51.9	1	26.1	1
B10	59.8	1.152	24.6	0.943
B11	103	1.98	23.5	0.90
B12	42.8	0.819	24.7	0.946
B13	42.5	0.819	22.9	0.877
B14	54.0	1.040	27.3	1.046
B15	52.7	1.015	26.6	1.019
B16	51.0	0.983	25.0	0.985

Figure (21) shows the load deflection relation at mid span with different thicknesses of web bracket plate for models B9, B12 and B13. The failure loads were equal to 26.1, 24.7 and 22.9 kN for plate thickness 3, 2.5 and 2 mm respectively, while the deflection were equal to 51.9 ,42.8 and 42.5 mm respectively. The failure happened due to local buckling of unstiffened channel for B9 as shown in Fig. (24) and buckling of gusset plate in beams B12and B13.

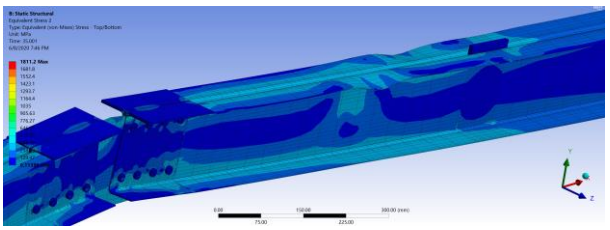

Fig.24. Buckling of Unstiffened Channel B9

Figure (22) shows the load-deflection curve for different bolt group for B9, B10and B11. The failure load were equal to 26.1, 24.6 and 23.5 kN for bolt group 4x2, 3x2 and 2x2 respectively. The deflection values were equal to 51.9, 59.8 and 103 mm respectively. The failure was bearing failure in unstiffened channel section for B10, B11 as shown in Fig. (25).

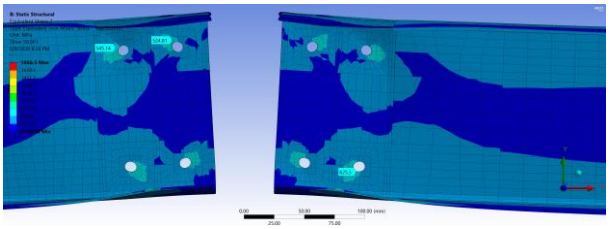

Fig.25. Bearing Failure of Channel Section B11

Figure (23) shows the load-deflection curve for different beams for B9, B14, B15 and B16 for different pretension force values. For the pretension loads equal to 20% and 40% the failure load increased by 4.6%, 1.9 % larger than non-pretensioned beam B1 respectively. The failure was happened due to the buckling of unstiffened channel section for B14, B15, and B16 as shown in Fig. (26).

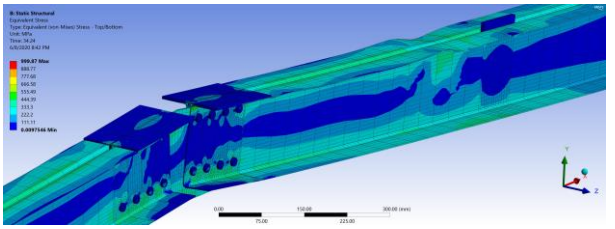

Fig.26. Buckling of Unstiffened Channel B14, B15 and B16

In order to assess the effectiveness of the bolted moment connections and allow direct comparison, a moment resistance ratio (Ψ) is established from the following equation:

$$\Psi = \frac{\textit{Calculated moment of a connection } (M1)}{\textit{Plastic moment capacity of connected section } (M2)}$$

The moment ratio-rotation curve, are plotted using the moment resistance ratio (Ψ) and the alternative beam rotation. The rotation (r) is calculated by the beam end rotation. The calculated moment (M1) was calculated from load step value and the alternative reaction and the plastic moment capacity (M2) for the two channels was calculated to be 17.59 kN.m according to the AISC specification.

The moment rotation curves for all modeled beams were presented in Figs. (27, 28 and 29) to compare the effect of plate thickness, bolt group dimension and pretension load for the two cases of connecting gusset plate shape respectively. The maximum moment ratio with the rotation value are listed in Table (7) for single gusset plate connection and listed in Table (8) for the case of double gusset plates.

The moment rotation curves show that all tested models are rotated linearly in primary step of applied loads, and then they exhibited to non-linear deformation characteristics when the stiffness of the connection decreased and the applied loads arrived to the failure load.

Table .7. Maximum Moment resistance and rotation Failure for single gusset plate

Model (NO)	Max Moment ratio (Ψ)	Failure rotation (r) (rad)
B1	0.72	0.022
B2	0.69	0.026
B3	0.67	0.040
B4	0.69	0.024
B5	0.67	0.035
B6	0.78	0.0266
B7	0.77	0.0266
B8	0.74	0.026

Table .8. Maximum Moment resistance and rotation Failure for double gusset plates

Model (NO)	Max Moment ratio (Ψ)	Failure rotation (r) (rad)
B9	0.74	0.026
B10	0.70	0.0299
B11	0.67	0.0514
B12	0.70	0.0214
B13	0.65	0.0213
B14	0.77	0.0277
B15	0.76	0.0264
B16	0.71	0.0255

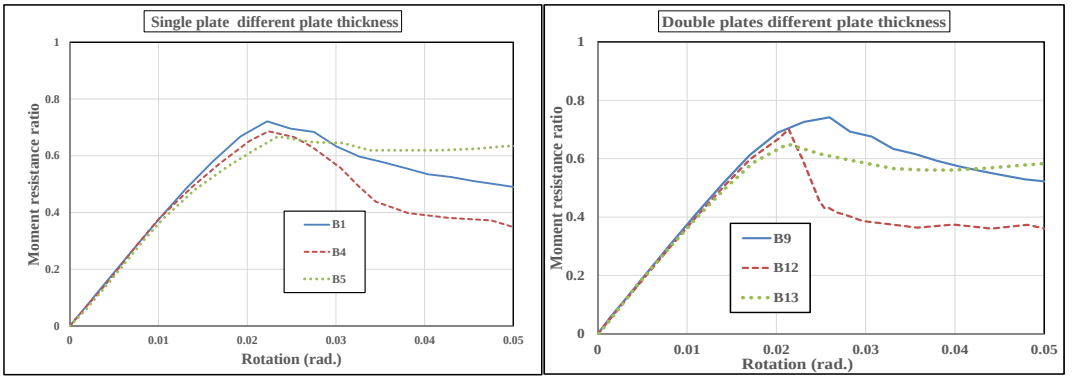

a) Moment Rotation Curve for single G.PL

b) Moment Rotation Curve for Double G.PL

Fig.27. Moment Rotation Curve for Different Gusset Plate Thickness

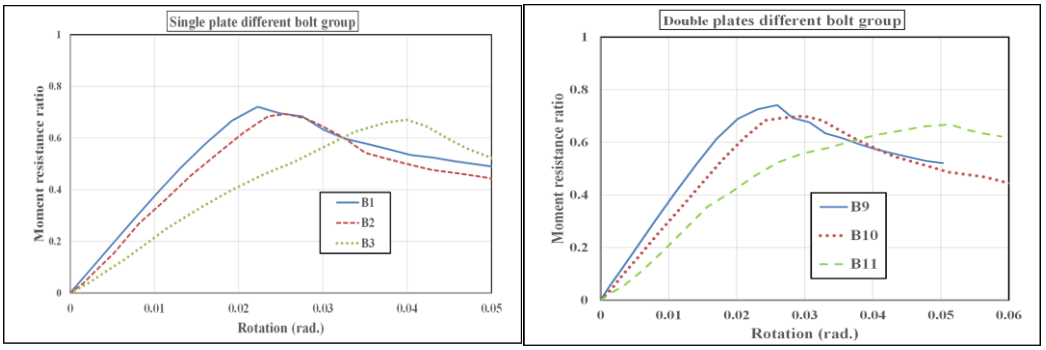

a) Moment Rotation Curve for single G.PL b) Moment Rotation Curve for Double G.PL

Fig.28. Moment Rotation Curve for Different Bolt group

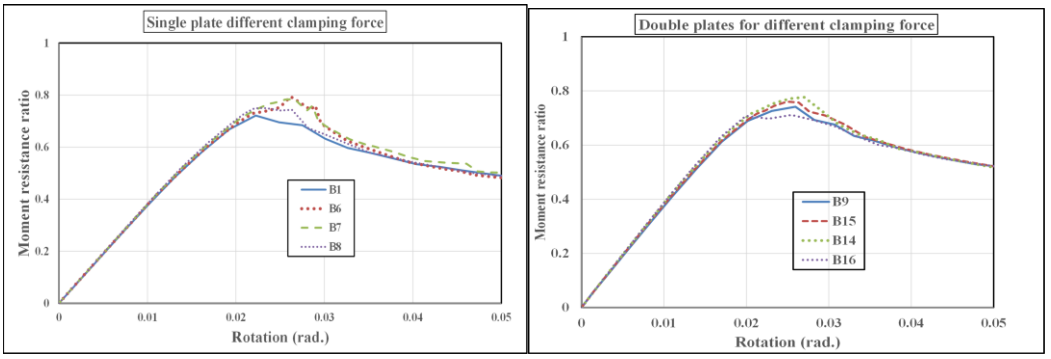

a) Moment Rotation Curve for single G.PL b) Moment Rotation Curve for Double G.PL

Fig.29. Moment Rotation Curve for Different Pretension Force Values

4. Discussion of the results

The previous curves showed that when using gusset plate thickness equal to the same thickness of channel section (beam) the failure occurs mainly in the gusset plate due to flexural failure of gusset plate while the moment resistance ratio at the failure position were found to be 0.67 and 0.65 in models B5 and B13 respectively. When increasing plate thickness by 25% w.r.t channel (beam) thickness the moment ratios were found to be 0.69 and 0.70 in models B4 and B12 respectively and the failure occurred due to the flexural failure of channel section. By increasing gusset plate thickness by 50% from channel thickness increasing the rigidity of the connection so the failure occurred in the channel section mainly and the moment ratios were found to be 0.72 and 0.74 in models B1 and B9 respectively.

In models B3 and B11 a bearing deformation was apparent in the bolt holes of the section web due to maximum moment acting at small lever arm for bolt group 2x2 with plate length equal to 5% from the beam length so the moment ratio were equal to 0.67 for the two models. The minimum gusset plate length give the minimum moment resistance of section and give maximum rotation of the beam.

In models B6, B7, B8, B14, B15 and B16 the failure occurs due to flexural failure of channel section and the corresponding moment resistance were ranges from to 0.71 to 0.78. Using of pretension

load of 20% increases the moment resistance of the connection by 6%and 3% from the moment ratio of non-pretension bolts for single and doubled gusset plate respectively. Increasing the pretension load value than 20% decreasing the moment resistance ratio due to local imperfection at bolts for thin thicknesses.

5. Conclusions

From the numerical study for cold formed moment connections some conclusions can be summarized as follows:

- Decreasing the length of gusset plate and the bolts number lead to increasing the maximum deflection and decreasing the failure load due to bearing failure around the bolt holes.
- Appling pretension load 20% increasing connection efficiency by 6% approximately from using non-pretension bolts.
- The connecting gusset plate thickness should not be less than 1.5 times of section thickness to insure that the failure is not occurring in the connection.
- Using gusset plate thickness equal to section thickness give moment resistance value equal to 0.65 due to flexural failure of gusset plate
- Finite element simulation for cold formed moment connection gives good predictions for deflection and maximum load.

References

[1] AISI (American Iron and Steel Institute) North American Specification for The Design of Cold-Formed Steel Structural Members. AISI S100. Washington, DC: AISI, 2016.

[2] Cold-formed steel structure code AS/NZ 4600:1996.Sydney: Standards Australia/ Standards New Zealand; 1996.

[3] ANSYS; ANSYS Workbench Release 19.2 ANSYS, Inc. Products Release 19.2 ; http://www.ansys.com.

[4] British Standards Institution.1998, BS595 : Structural Use of Steel Work in Buildings: part5:Code of practice for the design of cold-formed sections .London ,UK.

[5] J.B.P. Lim and D.A. Nethercot, “Ultimate Strength of Bolted Moment-Connections Between Cold-Formed Steel Members”, Thin-Walled Structures Vol. 41, pp. 1019-1039, 2003.

[6] D. Dubina, and R. Zaharia, “Cold-Formed Steel Trusses with Semi-Rigid Joints”, Thin-Walled Structures Vol. 29, Nos 1-4, pp.273-287,1997.

[7] D. Dubina,” Structural Analysis and Design Assisted by Testing of Cold-formed Steel Structures”.Thin-Walled Structures Vol. 46, pp. 741-764, 2008.

[8] M. Dundu and A.R. Kemp ,“Strength Requirements of Single Cold-Formed Channels Connected Back-to-Back” J. Constr. Steel Res Vol. 62, pp. 250-261, 2006.

[9] KF. Chung, “Building Design Using Cold Formed Steel Sections: Worked Examples to BS5950: part 5: 1987”, The Steel Construction Institute, 1993.

[10] WK. Yu, KF. Chung and MF. Wong, “Analysis of Bolted Moment Connection In Cold Formed Steel Beam–Column Sub-Frame”, J Construction Steel Res Vol. 61, No 9, pp. 1332-1352, 2005.

[11] KF. Chung, WK. Yu and AJ. Wang, “Structural Performance of Cold Formed Steel Column Bases with Bolted Moment Connections”, Steel Compos Struct Vol. 5, No 4 pp. 289-304, 2005.

[12] KF. Chung and L. Lau,“Experimental Investigation on Bolted Moment Connections among Cold-Formed Steel Members”, Eng. Struct. Vol. 21, No 10 pp. 898-911,1999.

[13] GJ. Hancock, “Design of Cold-Formed Steel Structures. 3rd ed Australian Institute of Steel Construction”; 1998.

[14] B.A. Ali, S. Saad, M.H.Osman and Y. Ahmed,“Finite Element Analysis of Cold-Formed Steel Connections”, International Journal of Engineering (IJE) Vol. 5 , Issue 2, 2011.

[15] A. B. Sabbagh, M. Petkovski, K. Pilakoutas and R. Mirghaderi, “Ductile Momemt-Resisting Frames Using Cold-Formed Steel Sections:An Analytical Investigation” , Journal of Constructional Steel Research Vol. 67, pp. 634-646, 2011.

[16] L. H. Tev and V. Yazici, “Shear Lag and Eccentricity Effect of Bolted Connections in Cold-formed Steel Sections”, Engineering Structures Vol. 52 , pp. 536-544, 2013.

[17] J. B.P. Lim, J . Gregory , g. C. Clifton, C. H. Pha, and D. Raj, “DSM for Ultimate Strength of Bolted Moment - Connections Between Cold-Formed Steel Channel Members”, Journal of Constructional Steel Research Vol. 117, pp.196-203, 2016.

[18] K. Rinchen and J.R. Rasmussen, “Behaviour and Modelling of Connections in Cold-formed Steel Single C Section Portal Frames”, Thin-Walled Structures Vol. 143 ,106233, 2019.

[19] M. El Aghoury, E. Amoush, and M. Soliman, “Numerical Study of Bolted Moment Connections in Cold-Formed Steel Frames”, Future Engineering Journal Vol. 1 , 2314-7237,2020.